

# Integrated spectral energy distributions of binary star composite stellar populations

Zhongmu Li<sup>1,2</sup> <sup>\*</sup>, Liyun Zhang<sup>3</sup>, Jinzhong Liu<sup>4</sup>

<sup>1</sup>*Institute for Astronomy and History of Science and Technology, Dali University, Dali 671003, China*

<sup>2</sup>*Key Laboratory of Optical Astronomy, National Astronomical Observatories, Chinese Academy of Sciences, Beijing 100012, China*

<sup>3</sup>*College of Science/Department of Physics@NAOC-GZU-Sponsored Center for Astronomy Research, Guizhou University, Guiyang 550025, China*

<sup>4</sup>*Xinjiang Astronomical Observatory, Chinese Academy of Sciences, Urumqi 830011, China*

Accepted 1988 December 15. Received 2011 December 14; in original form 1988 October 11

## ABSTRACT

This paper presents theoretical integrated spectral energy distributions (SEDs) of binary star composite stellar populations (bsCSPs) in early-type galaxies, and how the bsCSP model can be used for spectral studies of galaxies. All bsCSPs are built basing on three adjustable inputs (metallicity, ages of old and young components). The effects of binary interactions and stellar population mixture are taken into account. The results show some UV-upturn SEDs naturally for bsCSPs. The SEDs of bsCSPs are affected obviously by all of three stellar population parameters, and the effects of three parameters are degenerate. This suggests that the effects of metallicity, and the ages of the old (major in stellar mass) and young (minor) components of stellar populations should be taken into account in SED studies of early-type galaxies. The sensitivities of SEDs at different wavelengths to the inputs of a stellar population model are also investigated. It is shown that UV SEDs are sensitive to all of three stellar population parameters, rather than to only stellar age. Special wavelength ranges according to some SED features that are relatively sensitive to stellar metallicity, young-component age, and old-component age of bsCSPs are found by this work. For example, the shapes of SEDs with wavelength ranges of 5110–5250 Å, 5250–5310 Å, 5310–5350 Å, 5830–5970 Å, 20950–23550 Å are relatively sensitive to the stellar metallicity of bsCSPs. The shapes of SEDs within 965–985 Å, 1005–1055 Å, 1205–1245 Å are sensitive to old-component age, while SED features within the wavelength ranges of 2185–2245 Å, 2455–2505 Å, 2505–2555 Å, 2775–2825 Å, 2825–2875 Å to young-component age. The results suggest that some line indices within these special wavelength ranges are possibly better for stellar population studies compared to the others, and greater weights may be given to these special SED parts in the determination of the stellar population parameters of early-type galaxies from fitting SEDs via bsCSPs.

**Key words:** techniques: spectroscopic — galaxies: fundamental parameters — galaxies: stellar content

## 1 INTRODUCTION

Integrated spectral energy distribution (SED) is one of the most important tools for studying early-type galaxies. It can be used to investigate a lot of physical information of galaxies, because SEDs at different wavelengths are usually dominated by different physical parameters. For example, SED fitting can give insight to stellar mass, age, metallicity, and redshift of galaxies. On studies of SEDs of galaxies, one can use both observational spectral templates or theoretical SEDs. When theoretical SEDs are taken for studying the

stellar populations of early-type galaxies, many evolutionary stellar population synthesis models, e.g., Leitherer et al. (1999) and Vázquez et al. (2007) (Starburst99), Vazdekis (1999), Schulz et al. (2002), Cerviño et al. (2002), Robert et al. (2003), Bruzual & Charlot (2003) (BC03), Le Borgne et al. (2004) (PEGASE-HR), Maraston (2005) (M05), Lançon et al. (2008), Mollá et al. (2009), are usually used. However, all of these models are single star simple stellar population (ssSSP) models, which do not take the effects of binary evolution and population mixture into account. Meanwhile, observations in the Galaxy show that more than a half of stars are in binaries. Studies on the evolution of binary stars show that binary stars

<sup>\*</sup> E-mail: zhongmu.li@gmail.com

have significantly different evolution processes comparing to single stars. When binary stars are used to model the SEDs of stellar populations of early-type galaxies, some recent studies show that binary evolution can affect number or spectral population synthesis studies significantly (van Bever et al. 1999; Van Bever & Vanbeveren 2003; Li & Han 2008a,b, 2009; Li et al. 2010; Zhang et al. 2010; Han et al. 2010), especially in the UV (e.g., Belkus et al. 2003), X-ray (Van Bever & Vanbeveren 2000), and optical bands (Han et al. 2007). Therefore, it is necessary to model the SEDs of galaxies via binary stars. In addition, a lot of works (e.g., Mármol-Queraltó et al. 2009) showed that galaxies, even early-type ones, should undergo more than one star bursts. It means that there are multiple stellar populations in early-type galaxies. This calls for composite stellar population (CSP) models instead of simple stellar population (SSP) models to give more detailed SED studies to early-type galaxies. Han et al. (2007) studied the UV-upturn of SEDs of elliptical galaxies via binary stars, but all populations are assumed the solar metallicity ( $Z = 0.02$ ). Because many works show wide metallicity ranges for early-type galaxies, it is necessary to study the SEDs of early-type galaxies using a more advanced binary star composite stellar population (bsCSP) model, which covers a large metallicity range. This paper presents a new model, via assuming an old (major in stellar mass) and a young (minor) SSP component for a bsCSP. The assumption of two populations for a bsCSP is taken because early-type galaxies have relatively simple star formation histories comparing to other galaxies, and it is possible to give the main information of stellar populations of early type-galaxies via two stellar population components. Our work aims to investigate how model inputs affect the SEDs of populations and to find the sensitivities of different parts of SEDs to model inputs.

The paper is organized as follows. In Sect. 2, we introduce the binary star composite stellar population model. In Sect. 3, we study how different inputs of a bsCSP model affect the SEDs of populations. In Sect. 4, we study the sensitivities of SEDs at different wavelengths to three main parameters of a bsCSP. In Sect. 5, the bsCSP model is used to determine some important parameters of three elliptical galaxies. Finally, we give our conclusion and discussion in Sect. 6.

## 2 BINARY STAR COMPOSITE STELLAR POPULATION MODEL

There are two steps to build the SEDs of bsCSPs. First, a large database of SEDs of binary star simple stellar populations (bsSSPs) is built. Stars in a bsSSP are assumed to form at a star burst and have the same metallicity. Second, the SEDs of bsCSPs are built on the basis of the SED database of bsSSPs. Because there is no common results for the stellar mixture of galaxies, we take a simple way to model bsCSPs. Each bsCSP is assumed to contain a pair of old and young components with the same metallicity. This assumption is in agreement of previous studies that early-type galaxies are dominated by old populations and there is only a little fraction of young population in such galaxies. The mass fraction of young component is assumed to be dependent on

the ages of two components of bsCSPs, which is calculated by formula (1). This means that the mass fraction of young component declines exponentially with increasing difference between the ages of old and young components. This is in agreement with some previous studies on the star formation histories of early-type galaxies, e.g., Thomas et al. (2005).

$$F_2 = 0.5 \exp\left[\frac{t_2 - t_1}{\tau}\right] \quad (1)$$

where  $F_2$  is the mass fraction of young component;  $t_1$  and  $t_2$  are the ages of the old and young components of a bsCSP. As a standard model,  $\tau$  is taken as 3.02, according to the observational fraction of bright early type galaxies with recent ( $\leq 1$  Gyr) star formation at a level more than 1%-2% (Yi et al. 2005; Li & Han 2007).

The important ingredients and specialties of our model are as follows. An initial mass function (IMF) of Chabrier (2003) with lower and upper mass limits of 0.1 and 100  $M_\odot$  respectively is taken for bsCSPs. The evolution of binaries is calculated via the rapid stellar evolution code of Hurley et al. (2002) (hereafter Hurley code), so that most of binary evolution processes such as mass transfer, mass accretion, common-envelope evolution, collisions, supernova kicks and angular momentum loss are included. Different mass transfer mechanisms, i.e., dynamical mass transfer, nuclear mass transfer and thermal mass transfer are taken into account using the results of many works (e.g., Tout et al. 1997; Hjellming & Webbink 1987). One can see Hurley et al. 2002 for more details. According to a previous work, in all binary interactions, Roche lobe overflow (RLOF) and common envelope (CE) may affect the formation of hot subdwarfs and then the UV spectra of stellar populations more significantly (Han et al. 2007).

The default values in Hurley code, i.e., 0.5, 1.5, 1.0, 0.0, 0.001, 3.0, 190.0, 0.5, and 0.5, are taken for wind velocity factor ( $\beta_w$ ), Bondi-Hoyle wind accretion fraction ( $\alpha_w$ ), wind accretion efficiency factor ( $\mu_w$ ), binary enhanced mass loss parameter ( $B_w$ ), fraction of accreted material retained in supernova eruption ( $\epsilon$ ), common-envelope efficiency ( $\alpha_{CE}$ ), dispersion in the Maxwellian distribution for the supernovae kick speed ( $\sigma_k$ ), Reimers coefficient for mass loss ( $\eta$ ), and binding energy factor ( $\lambda$ ), respectively. Although the above default values remain somewhat large uncertainties, the results for spectral stellar population synthesis will be not affected too much by the uncertainties of these parameters. We test the effects of uncertainties in these parameters by comparing four modes with different input values. For convenience, the mode of stellar evolution by taking the default values will be cited as default mode hereafter. Then the evolutionary results of other three modes (A, B and C) are compared to that of the default mode. In mode A, we take the lowest values for all parameters (i.e., 0.125, 0.0, 0.0, 0.0, -1.0, 0.5, 0.0, 0.0 for  $\beta_w$ ,  $\alpha_w$ ,  $\mu_w$ ,  $B_w$ ,  $\epsilon$ ,  $\alpha_{CE}$ ,  $\sigma_k$  and  $\eta$ , respectively) to evolve 5000 binaries with metallicities ( $Z$ ) of 0.01, 0.02, and 0.03 from zero-age main sequence (ZAMS) to 15 Gyr, with an age interval of 0.1 Gyr. Then we compared the effective temperature ( $T_{\text{eff}}$ ) and surface gravity ( $\log g$ ) of stars in mode A to those obtained in the default mode. It shows that the two main stellar parameters ( $T_{\text{eff}}$  and  $\log g$ ) change only 0.20% on average when taking mode A instead of default mode. Then in mode B, similar to mode A, but the largest or large (for  $\sigma_k$ ) values are taken for all param-

ters (i.e., 7.0, 2.0, 1.0,  $1.0^6$ , 1.0, 10.0, 570.0, 2.0 for  $\beta_w$ ,  $\alpha_w$ ,  $\mu_w$ ,  $B_w$ ,  $\epsilon$ ,  $\alpha_{CE}$ ,  $\sigma_k$  and  $\eta$ , respectively) when evolving binaries. It shows that the average change of stellar parameters is 0.48% compared to the default mode, which is larger than in mode A. In the third mode, i.e., mode C, we set some random values to evolve 5000 binaries. The values for  $\beta_w$ ,  $\alpha_w$ ,  $\mu_w$ ,  $B_w$ ,  $\epsilon$ ,  $\alpha_{CE}$ ,  $\sigma_k$ , and  $\eta$  are set as 3.0, 1.0, 0.3, 100.0, 0.5, 5.0, 300.0 and 0.7, respectively. This mode shows an average change in stellar parameters of 0.35% compared to the default mode. Because the fitted formulae used by Hurley code to evolve stars can lead to uncertainties up to about 5% (Hurley et al. 2002), the changes of stellar evolutionary results that are caused by the uncertainties in the default parameters, are much less than the uncertainties result from using fitted formulae to evolve stars. Therefore, we conclude that the uncertainties in the default values of Hurley code will not change the main results of statistical studies like spectral stellar population synthesis. Thus we take the default values of Hurley code to evolve all stars in this work. Note that 3.0 is taken for  $\alpha_{CE}$  here also because it can produce enough double-degenerates while a widely used value of 1.0 can not when Hurley et al. (2002) tried to check the effects of input parameters of Hurley code via population synthesis of birth rates and Galactic numbers of the various types of binary.

When generating the star sample of populations, an uniform distribution is taken for the ratio ( $q$ , 0–1) of the mass of the secondary to that of the primary (Mazeh et al. 1992; Goldberg & Mazeh 1994), and the mass of the secondary is then calculated from  $q$  and the primary mass, where the mass of the primary is generated via a Monte Carlo technique according to the selected IMF. The separation ( $a$ ) of two components of a binary is generated following the assumption that the fraction of binary in an interval of  $\log(a)$  is constant when  $a$  is big ( $10R_\odot < a < 5.75 \times 10^6 R_\odot$ ) and it falls off smoothly when  $a$  is small ( $\leq 10R_\odot$ ) (Han et al. 1995), which can be written as

$$a \cdot p(a) = \begin{cases} a_{\text{sep}}(a/a_0)^\psi, & a \leq a_0 \\ a_{\text{sep}}, & a_0 < a < a_1 \end{cases} \quad (2)$$

where  $a_{\text{sep}} \approx 0.070$ ,  $a_0 = 10R_\odot$ ,  $a_1 = 5.75 \times 10^6 R_\odot$  and  $\psi \approx 1.2$ . An uniform distribution is taken for the eccentricity ( $e$ ) of each binary system. Most binary interactions, e.g., mass transfer, common-envelope evolution, collisions, and tidal interactions, are taken into account in the bsCSP model. The fraction of binary stars in each population (4000000 single stars) is taken as the typical value of the Galaxy, i.e., 50%. When calculating the SEDs of stellar populations, the BaSeL 3.1 spectral library (Lejeune et al. 1997, 1998; Westera et al. 2002) is used because of its wide wavelength coverage and reliability. On average, the spectral library leads to about 3% uncertainties in the final SEDs of bsCSPs.

### 3 EFFECTS OF MODEL INPUTS ON SEDS

#### 3.1 Effect of stellar metallicity

Most previous works took the solar metallicity for studying the SEDs of early-type galaxies, especially elliptical galaxies, but stellar metallicities ( $Z$ ) of early-type galaxies dis-

tribute in a large range (e.g., 0.005 – 0.05, Gallazzi et al. 2005). Therefore, it is interesting to investigate how stellar metallicity changes the SEDs of stellar populations of early-type galaxies. The effects of metallicity on the SEDs of bsCSPs are investigated in this section. Figs. 1 and 2 show some results. In each panel of the two figures, the SEDs of bsCSPs with different metallicities but the same pair of old and young-component ages are compared. Symbols ‘ $t_1$ ’ and ‘ $t_2$ ’ denote the ages of old and young-components, respectively. As can be seen, stellar metallicity affects the SEDs of bsCSPs significantly. In particular, UV SED is shown to be very sensitive to stellar metallicity. When stellar metallicity changing from 0.004 to 0.03, the logarithmic flux in UV band can change as large as 1.8 dex. Even stellar metallicity changes only from 0.2 to 0.01, the UV spectra of a bsCSPs can change a lot for most of stellar populations. This suggests that stellar metallicity should be taken into account when explaining the UV spectra of early-type galaxies. In addition, the result shows no well-regulated correlation between metallicity and the change of SEDs of bsCSPs, comparing to a solar metallicity case. Therefore, it is useful to use bsCSPs with metallicities in a wide range to study the SEDs of early-type galaxies.

#### 3.2 Effect of old-component age

This section investigates how the age of old component,  $t_1$ , affects the SED of bsCSPs. As examples, some stellar populations with metallicities of 0.01, 0.02, and 0.003 are investigated. The ages of young components of bsCSPs are taken as 1, 2, 3, or 5 Gyr, and the ages of old components differ from 13 to 5 Gyr. The main results are shown in Figs. 3 to 5. It is found that the age of old component affects the SEDs of bsCSPs obviously. The optical and near-infrared flux decreases with increasing old-component age ( $t_1$ ), for fixed metallicity ( $Z$ ) and young-component age ( $t_2$ ). However, the flux and shape of UV-band SEDs of bsCSPs do not change with  $t_1$  regularly. It seems that UV SED is not only sensitive to the old-component age of bsCSPs.

#### 3.3 Effect of young-component age

The effects of the age of the young component,  $t_2$ , on the SEDs of bsCSPs is investigated in this section. As examples, three stellar metallicities (0.01, 0.02, and 0.03) and four ages (5, 8, 10, and 13 Gyr) are taken for the stellar metallicity and old-component age of bsCSPs, respectively. The results are shown in Figs. 6 to 8. It is found that the age of young component has no obvious effect on SEDs, when the young components of bsCSPs are older than 2 Gyr. However,  $t_2$  affects the SEDs of bsCSPs significantly when  $t_2$  is less than 2 Gyr. In detail, the change of logarithmic flux of UV SED of bsCSP can be as large as 2 dex, when  $t_2$  changes in a wide range, e.g., 0.5–10 Gyr. In addition, it is found that the younger the young component, the larger the flux in UV band, for bsCSPs with the same metallicity ( $Z$ ) and old-population age ( $t_1$ ). In addition, the three figures show that the shape of SED does not change obviously for wavelength shorter than about 1000 Å, when  $t_2$  changes from  $t_1$  to 0.5 Gyr. Meanwhile, the shape of SED from 1000 to 3000 Å is affected by  $t_2$  more obviously. This confirms that the

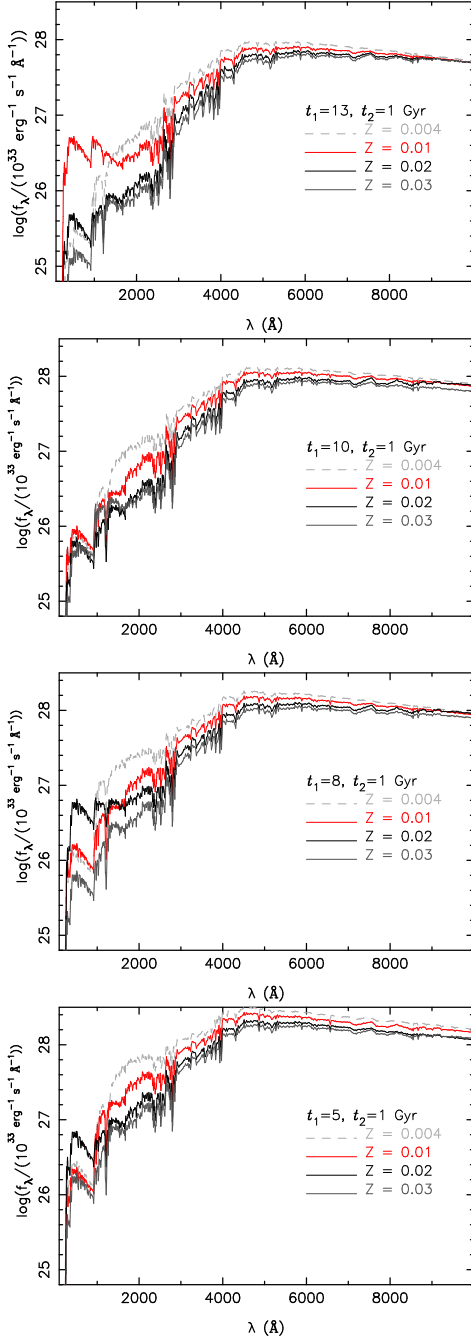


**Figure 1.** Comparison of SEDs of bsCSPs with different stellar metallicities. All bsCSPs have the same age for their young components, i.e.,  $t_2 = 1$  Gyr. The ages of old-components of bsCSPs,  $t_1$ , are set to be different from 13 to 5 Gyr in each panel. Stellar populations with different metallicities are shown in various colours as the remarks in each panel.

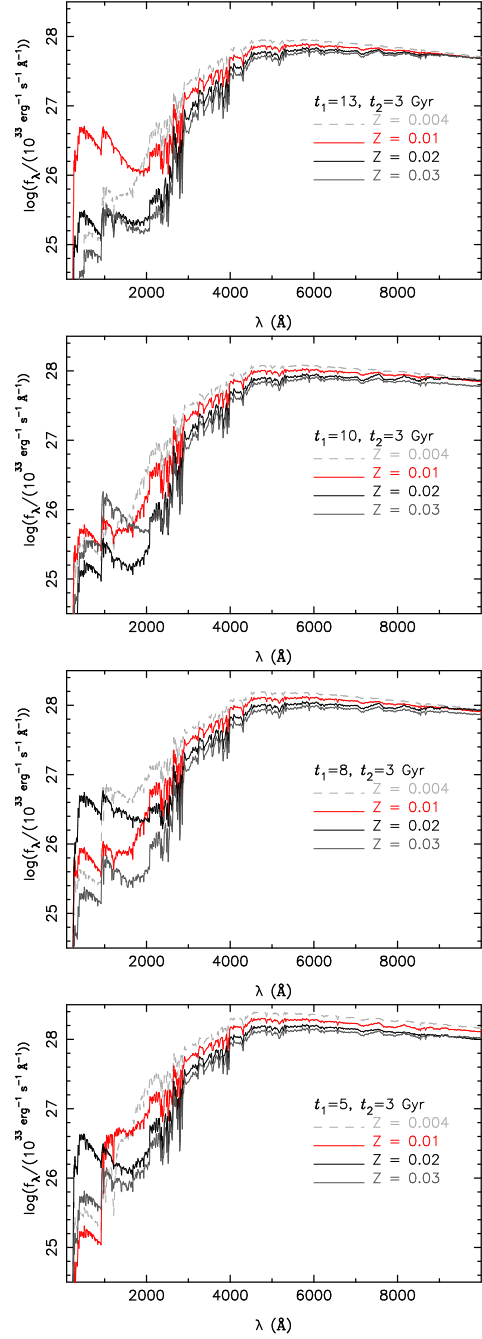


**Figure 2.** Similar to Fig. 1, but for bsCSPs with a young-component age of 3 Gyr.

#### 4 SENSITIVITIES OF SEDS TO STELLAR POPULATION MODEL INPUTS

Because three input stellar population parameters (metallicity, old and young-component ages) have some effects on the SEDs of bsCSPs, it is difficult to find SED features for determining each parameter from the results shown in Section 3. We investigate the sensitivities of SEDs to three main input parameters of bsCSPs. The absolute sensitivity to an input stellar population parameter is defined as the average change of logarithmic flux ( $\log f_\lambda$ ) at a wavelength, when the input parameter changes by 10% (0.0026 for  $Z$ , 0.7 Gyr for old-component age, and 0.6 Gyr for young-component

SED within a wavelength range of 1000 to 3000 Å is sensitive to the age of young component. This agrees to many previous works, e.g., Yi et al. (1999) and Han et al. (2007).

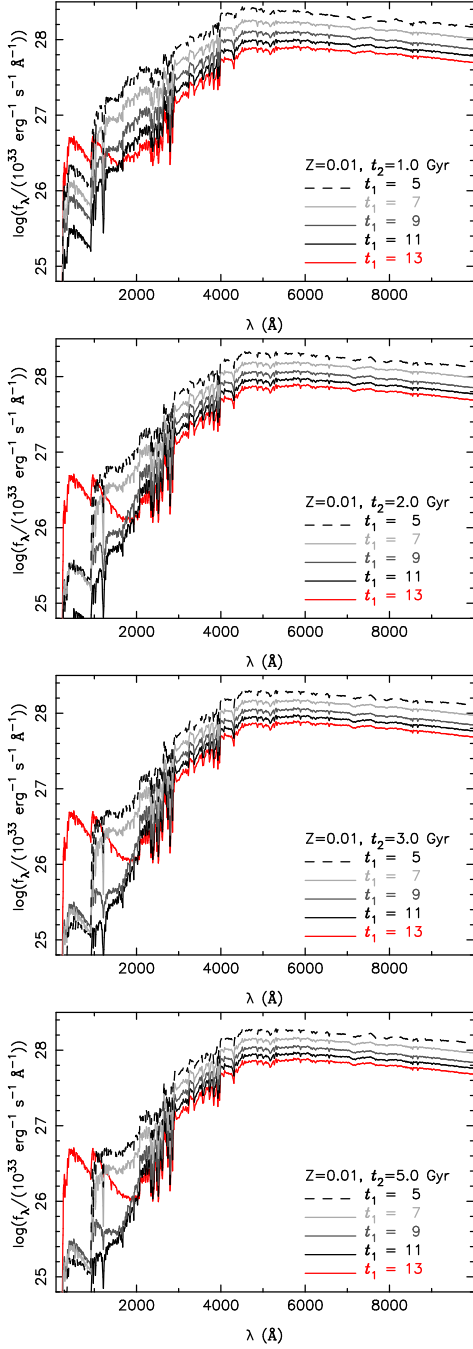


**Figure 3.** Comparison of SEDs of bsCSPs with different old-component ages. The ages of old-components of bsCSPs,  $t_2$ , are set to be different (1, 2, 3, 5 Gyr) in four panels, while the stellar metallicity,  $Z$ , is set to be the same. Stellar populations with different old-component ages are shown in various colours or line types.

age) within its possible range. The absolute sensitivities are calculated using the SEDs of bsCSPs with 4 metallicities (0.004, 0.01, 0.02, and 0.03) and 8 old-component ages (from 5 to 12 Gyr with a 1 Gyr interval). The ages of young components of bsCSPs take different values from its old-component age to 1 Gyr. Note that because this work aims to study the SEDs of early-type galaxies, the possible ranges for the metallicities and old-component ages are taken from a re-

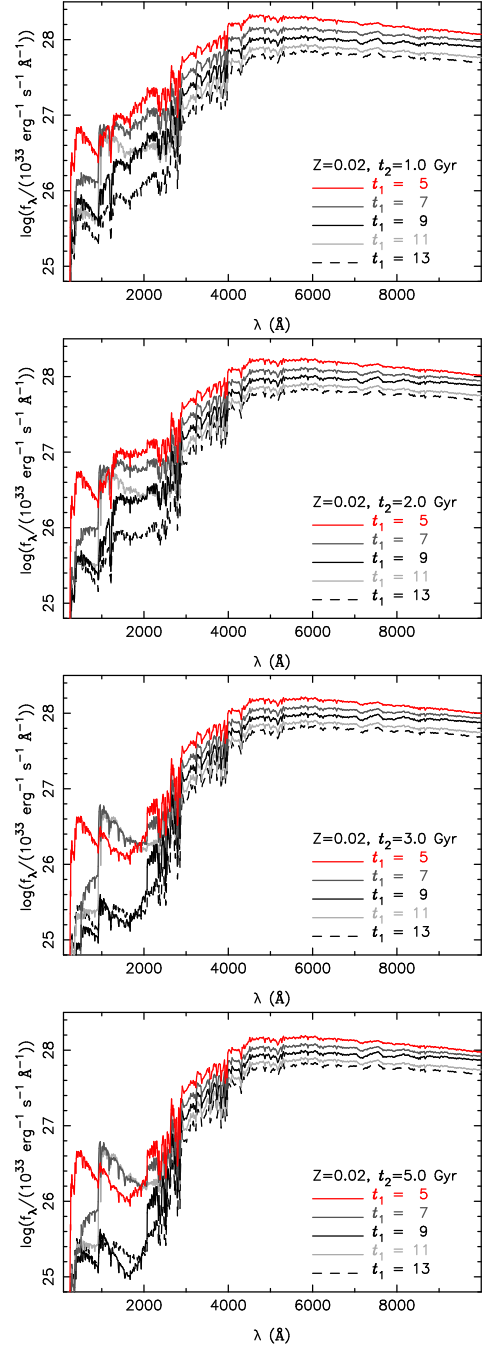


**Figure 4.** Similar to Fig. 3, but for bsCSPs with a solar metallicity. Note that the meanings of colours and line types in this figure are different from those in Fig. 3.

sult of stellar population study of nearby early-type galaxies (e.g., Gallazzi et al. 2005).

The absolute sensitivities at all wavelengths are shown in Fig. 9. It is found that the sensitivities to three stellar population parameters differ a lot at various wavelengths. As a whole, SEDs in near infrared and infrared bands ( $\lambda \geq 8000$  Å) are more sensitive to old-component age, while UV band SED is sensitive to all of three stellar population parameters. In other words, old-component age affects the brightness in near infrared and infrared bands, significantly. The brightness in UV band is affected by all of three stellar

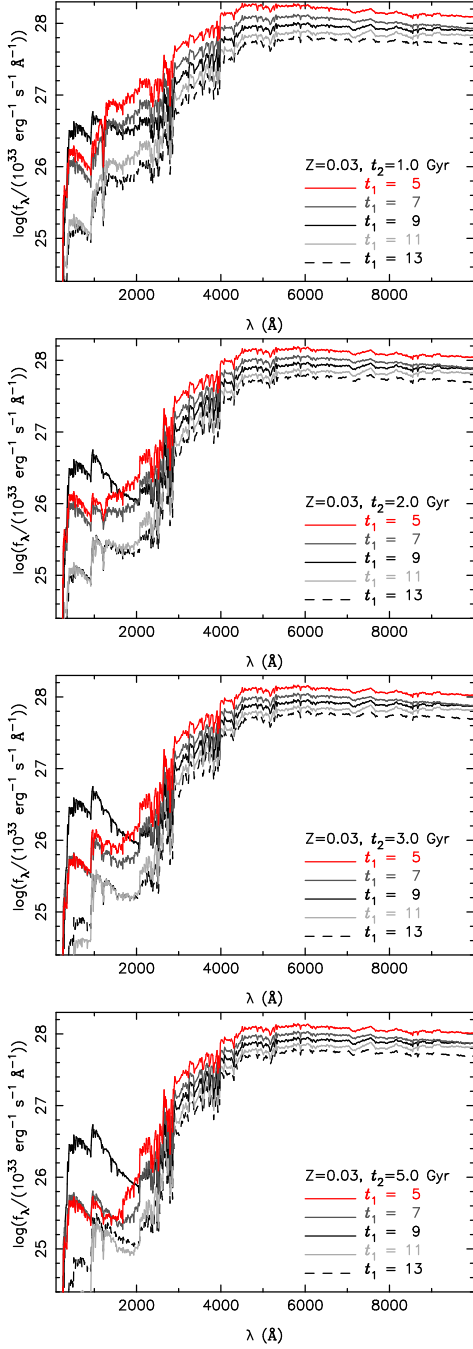


**Figure 5.** Similar to Figure 3, but for bsCSPs with a metallicity ( $Z$ ) of 0.03. Colours and line types have different meanings comparing to Fig. 3.

population parameters. As we see, UV flux is affected by stellar metallicity significantly. The optical SEDs of bsCSPs are less sensitive to the age of young components, compared to the stellar metallicity and age of old components of bsCSPs. This suggests that it is difficult to determine the young-component ages of bsCSPs via optical SEDs. Therefore, the results suggest to use multiple-band SEDs for well determining the stellar metallicity, old-component and young-component ages of early-type galaxies, via fitting SEDs.

Although Fig. 9 tells us the absolute changes in SEDs caused from 10 percent change of stellar metallicity, old-

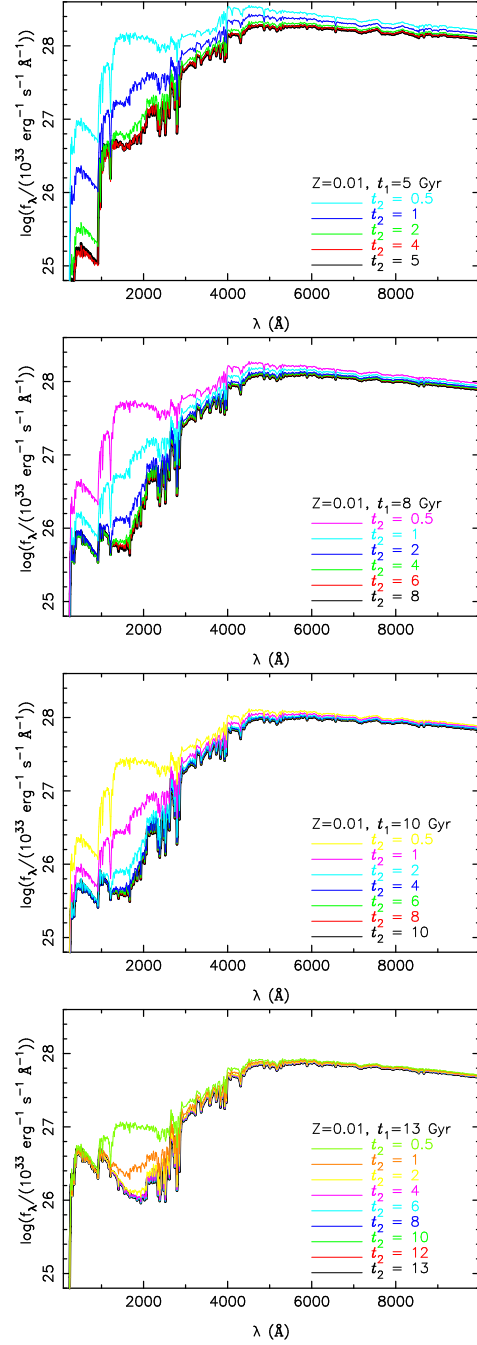


**Figure 6.** Comparison of SEDs of bsCSPs with the same metallicity and old-component age, but various young-component ages. In each panel, bsCSPs with various young-component ages are shown in different colours. Note that colours have different meanings in four panels.

component age, or young-component age, it is difficult to guide many of our studies. The reason is that usually we determine the stellar population parameters via fitting some relative spectral features (or shapes) of galaxies. Such special spectral features can be found by searching for the abrupt changes with wavelength of the relative sensitivities of SEDs to three stellar population parameters. For convenience, we use relative sensitivities instead of absolute sensitivities here. The relative sensitivities of SEDs to stellar

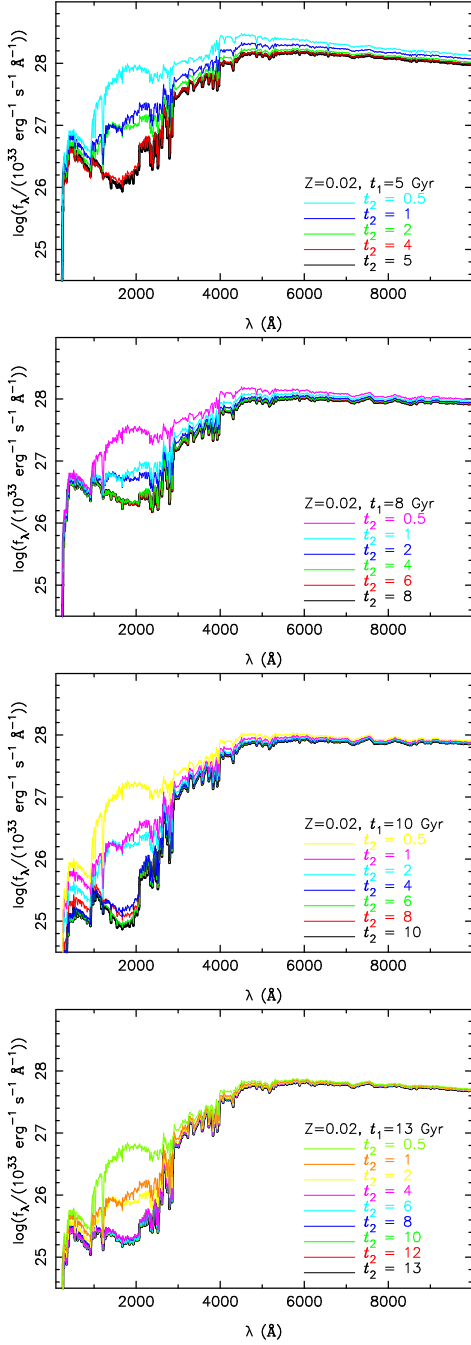


**Figure 7.** Similar to Figure 6, but for bsCSPs with a solar metallicity ( $Z = 0.02$ ).

metallicity is obtained by dividing absolute sensitivities to metallicity by 1.2. The relative sensitivities of SEDs to old-component age and young-component age are obtained by dividing absolute sensitivities by 0.7. This makes the maximum of relative sensitivities of SEDs to three stellar population parameters equal to 1 for  $\lambda > 500 \text{ \AA}$ . Then some spectral features can be found from the relative sensitivities. For example, if the sensitivity to old-component age within a special wavelength range is significantly larger than in neighborhood, while the sensitivities to stellar metallicity and young-component age in the same wavelength range do not have similar trend, the SED feature within the given

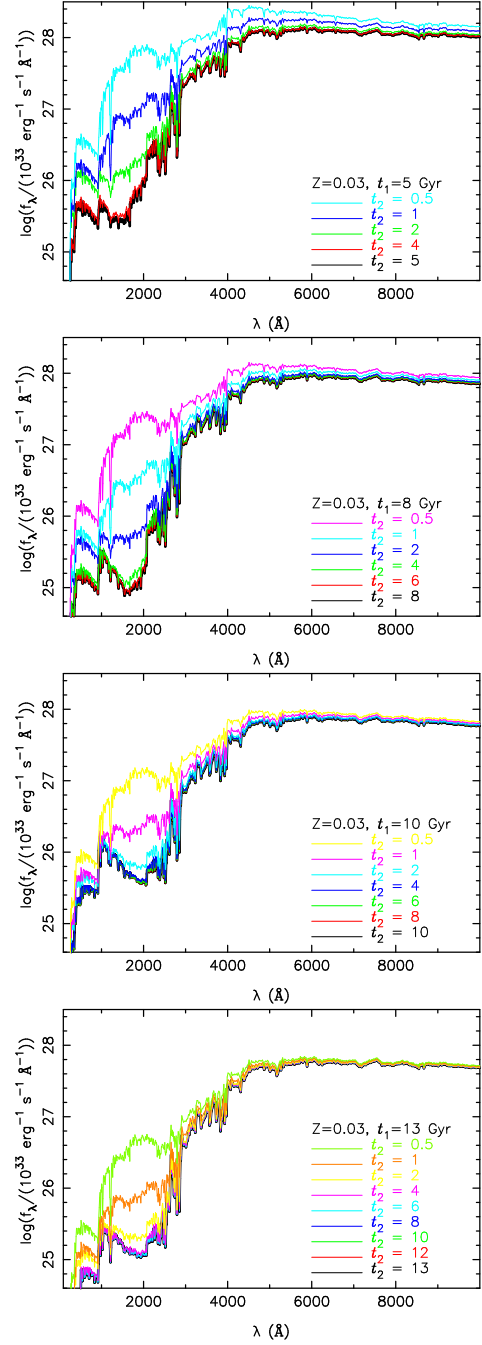


**Figure 8.** Similar to Figure 6, but for bsCSPs with a metallicity ( $Z$ ) of 0.03.

wavelength range is relatively sensitive to old-component age. It means the relative shape of SEDs within the given wavelength range can be used as an old-component age indicator. One can check the sensitivities of SEDs within 1205–1245  $\text{\AA}$  (peak at 1225  $\text{\AA}$ ) in Fig. 10 for well understanding our method. Some spectral features that are sensitive to stellar metallicity and young-component age are found in the same way. Fig. 10 shows the relative sensitivities of SEDs to three stellar population parameters and the central wavelengths of some example spectral features that are sensitive to stellar metallicity, old-component age, or young-component age of bsCSPs. In detail, the results show



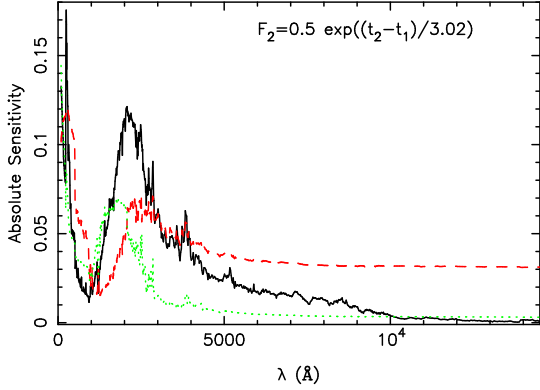


**Figure 9.** Absolute sensitivities of different SED parts to three stellar population parameters of bsCSPs. Black solid, red dashed, and green dotted lines show the sensitivities to metallicity, old-component age, and young-component age, respectively.

that SED features within wavelength ranges of 5110–5250 Å, 5250–5310 Å, 5310–5350 Å, 5830–5970 Å, 20950–23550 Å are relatively sensitive to stellar metallicity of bsCSPs. The SED features within 965–985 Å, 1005–1055 Å, 1205–1245 Å are sensitive to old-component age, while those within the wavelength ranges of 2185–2245 Å, 2455–2505 Å, 2505–2555 Å, 2775–2825 Å, 2825–2875 Å to young-component age.

It is found that although the UV SEDs of bsCSPs are related to all of three stellar population parameters, some spectral features (e.g.,  $1205 \leq \lambda \leq 1245$  Å) in UV band are found to be more sensitive to the old-component age. It is also found from Fig. 10 that SED features within 5110–5250 Å, 5250–5310 Å, 5310–5350 Å are relatively sensitive to stellar metallicity. This suggests that even bsCSP models instead of ssSSP models are used for studying the stellar populations of early-type galaxies, some widely used spectral line indices, e.g., Mg<sub>b</sub>, Fe5270, Fe5335, can be used as metallicity indicators. In addition, SED features in a wide wavelength range of near infrared band seem sensitive to stellar metallicity. It implies that infrared photometry has some potential for determining the stellar metallicity of galaxies. Moreover, it is shown that the age of young-components of bsCSPs of early-type galaxies can be estimated by some SED features within narrow wavelength ranges, e.g., 2775–2825 Å (with a peak wavelength of 2800 Å), because SEDs in these wavelength ranges are relative sensitive to young-component age of bsCSPs.

## 5 APPLICATION AND COMPARISON OF BSCSP MODELS TO GALAXIES

As a test, in this section we apply the above results, i.e., spectra database of bsCSPs and sensitivities of different spectral parts to the input stellar population parameters, to three elliptical galaxies, i.e., NGC1399, NGC1404, and NGC2865. Stellar population parameters of the three galaxies are determined via spectral fits. The observational spectra of three galaxies are taken from a database of UV-optical spectra of nearby quiescent and active galaxies, which was built by Storchi-Bergmann, Calzetti & Kinney ([http://www.stsci.edu/ftp/catalogs/nearby\\_gal/sed.html](http://www.stsci.edu/ftp/catalogs/nearby_gal/sed.html)), because of its convenience. Then the original spectra were

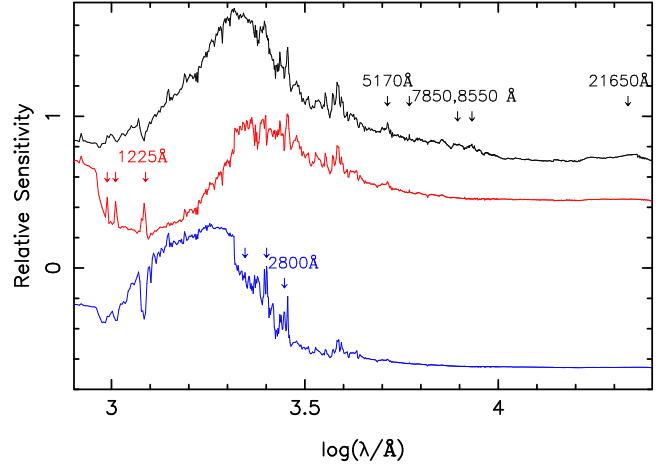


**Figure 10.** Relative sensitivities of different SED parts to three stellar population parameters of bsCSPs. Relative sensitivities to metallicity, and young-component age are added by 0.7 and -0.7 to make them separate from the sensitivities to old-component age. Black (top), red (mid), and blue (bottom) lines show the sensitivities to metallicity, old-component age, and young-component age, respectively.

degraded to fit the resolution of BaSeL 3.1 spectra. Some bsCSP models with metallicities of 0.0003, 0.001, 0.004, 0.01, 0.02 and 0.03 are used for fitting the observational spectra, and all spectra are normalized at 5510 Å. The range of old-population age of bsCSP models is 0.1–15 Gyr. Two methods are used to get the best fit results. In the first way, a homogeneous weight is given for almost all spectral parts. The spectral parts that have obvious uncertainties or poor quality in the observational spectra are given lower weights in all fits. The results show that NGC1399, NGC1404, NGC2865 have redshifts of 0.004753, 0.00650 and 0.008797, respectively. Their best fit stellar metallicities are shown to be 0.03, 0.03, and 0.01, respectively. Meanwhile, the best fit ages for the old and young populations in NGC1399, NGC1404 and NGC2865 are (11.8 and 10.9 Gyr), (10.3 and 1.7 Gyr) and (14.7 and 1.1 Gyr), respectively. When various weights are given to different spectral parts in the second way, the best fit stellar populations of NGC1399 and NGC1404 are shown to be different. The metallicity of NGC1404 is shown to be 0.02, instead of 0.03. NGC1399 is shown to include only an old (11.8 Gyr) population, while NGC1404 is shown to include a pair of populations with ages of 13.8 and 1.3 Gyr. The detailed comparison of the observed and best fit bsCSP spectra of the galaxies are shown in Figs. 11 and 12. Note that in the second way, four times weights are given to three spectral parts, i.e., 1205–1245 Å, 2775–2885 Å, 5110–5350 Å, according to their relative sensitivities to stellar population inputs. We see that the observational spectra of three elliptical galaxies can be fitted well using those of bsCSPs, as a whole. However, it is also seen that the spectral parts around 2000 and 3000 Å are not fitted well. This actually results from the poor quality of the observational spectra around 2000 and 3000 Å, because the part around 2000 Å is a overlap region of two observational spectra and the second order contamination of light causes uncertainties in the part of 3000–3200 Å. In addition, only bsCSPs with six metallicities are use for the



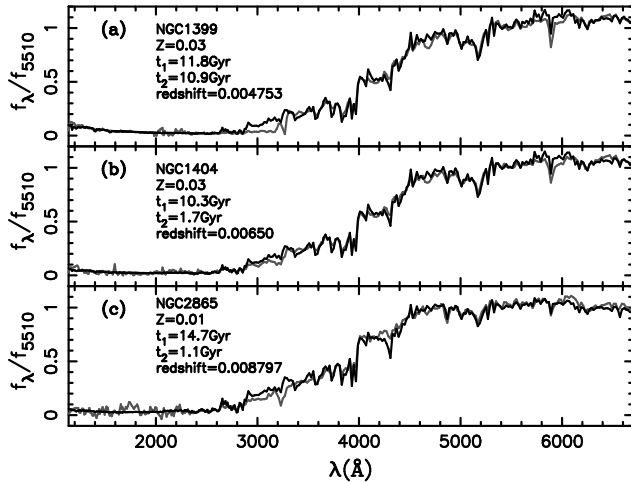


**Figure 11.** Comparison of observational and bsCSP fit spectra of three elliptical galaxies. All spectra are normalized at 5510 Å. Gray and black lines are for observational and theoretical spectra, respectively. The best fit redshifts and stellar population parameters can be seen in three panels. Homogeneous weight is given to all spectral parts in spectral fit. Note that the parts around 2000 and 3000 Å of observational spectra contains larger uncertainties.

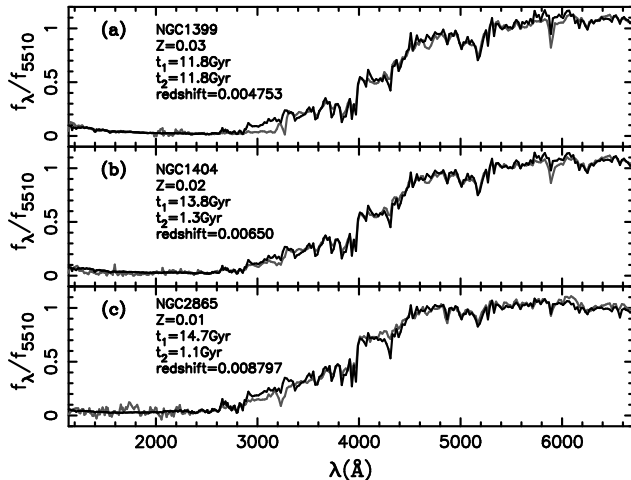


**Figure 12.** Similar to Fig. 11, but various weights are given to different spectral parts in the spectra fit according to the different relative sensitivities of various parts.

fit. This may also contribute to the differences between the observational and best fit spectra.

## 6 CONCLUSION AND DISCUSSION

Aiming to study the SEDs of early-type galaxies, this paper presents the SEDs of binary star composite stellar populations (bsCSPs) and studies the sensitivities of different parts of SEDs of bsCSPs to stellar metallicity, old-component and young-component ages. Some SEDs with UV-upturn are presented naturally for some bsCSPs. Our results also show detailed effects of three stellar population parameters on the SEDs of bsCSPs. It suggests that all of the three stellar population parameters should be taken into account in studies of SEDs of early-type galaxies.

In particular, this work shows clear effects of stellar metallicity on the UV SEDs of bsCSPs, even when metallicity changes within a range near the solar value, e.g., 0.01–0.03. Therefore, our results suggest to use bsCSPs with different metallicities for studying the SEDs of early-type galaxies, including studying UV-band SEDs. In addition, the results show that the flux in optical and infrared bands are dominated by the old-component age of bsCSPs, while the flux in UV band is affected by all of three stellar population parameters. However, it seems that metallicity determines the UV-band SEDs of bsCSPs, because it is much more sensitive to UV SED compared to the ages of two stellar population components. Our results suggest using multi-band SEDs to determine the stellar metallicity, old-component age, and young-component age of bsCSPs.

This work also showed some special wavelength ranges for studying bsCSPs of early-type galaxies. The results are potentially useful for determining the stellar metallicity, old-component age, and young-component age of bsCSPs of early-type galaxies via fitting relative spectral features (e.g., spectral line indices) of SEDs.

As a standard model, we take a formulae of  $F_2 = 0.5 \exp[(t_2 - t_1)/\tau]$  with  $\tau = 3.02$  for calculating the mass fraction of the young component of a bsCSP. The value of  $\tau$  affects the sensitivities of SED to the young-component age of bsCSPs obviously, because it changes the mass fractions of young-components of bsCSPs directly. We checked the sensitivities of SED to bsCSPs by taking different values (1, 2, 3.02 and 5) for  $\tau$ . The results showed that the bigger the value of  $\tau$ , the larger the sensitivity of UV-band SEDs to young-component age. However, the sensitivities of optical and infrared-band SEDs to the young-component age are always similar. The sensitivities of SEDs to metallicity and old-component age do not change obviously with different  $\tau$  values.

The initial mass function (IMF) of stellar populations can also affect the sensitivities of SED to stellar metallicity, old-component and young-component ages. However, even other IMFs are taken for building bsCSPs, the main results of this work will not change. This is checked using some bsCSPs with a Salpeter (1955) IMF. Therefore, the results of this paper can be used widely for stellar population studies. One can also refer to some works such as Conroy et al. (2009, 2010); Conroy & Gunn (2010) for better understanding the uncertainties in evolutionary population synthesis.

Because the stellar metallicity of most nearby early-type galaxies are shown to be higher than 0.004, we did not show the results for bsCSPs with lower metallicity. However, our study showed that if lower metallicities are taken for bsCSPs, their SEDs will change significantly. The effects of  $\alpha$ -element enhancement was not taken into account in this work, because the Hurley code can not evolve stars with  $\alpha$ -element enhancement. One can read recent papers, e.g., Lee et al. (2009) for reference.

## ACKNOWLEDGMENTS

We thank Profs. ZHAO Gang and SHI Jianrong for useful suggestions. We also thank Prof. Vanbeveren for comments and revision suggestions. This work has been supported by the Chinese National Science Foundation

(Grant Nos. 10963001, No. 10978010), Yunnan Science Foundation (No. 2009CD093), and Chinese Postdoctoral Science Foundation. Zhongmu Li gratefully acknowledges the support of Sino-German Center (GZ585) and K. C. Wong Education Foundation, Hong Kong. Liu's work was also supported by the light in China's Western Region (LCWR)(No.XBBS2011022).

## REFERENCES

- Belkus H., Van Bever J., Vanbeveren D., van Rensbergen W., 2003, *A&A*, 400, 429
- Bruzual G., Charlot S., 2003, *MNRAS*, 344, 1000
- Cerviño M., Mas-Hesse J. M., Kunth D., 2002, *A&A*, 392, 19
- Chabrier G., 2003, *ApJ*, 586, L133
- Conroy C., Gunn J. E., 2010, *ApJ*, 712, 833
- Conroy C., Gunn J. E., White M., 2009, *ApJ*, 699, 486
- Conroy C., White M., Gunn J. E., 2010, *ApJ*, 708, 58
- Gallazzi A., Charlot S., Brinchmann J., White S. D. M., Tremonti C. A., 2005, *MNRAS*, 362, 41
- Goldberg D., Mazeh T., 1994, *A&A*, 282, 801
- Han Z., Chen X., Zhang F., Podsiadlowski P., 2010, in G. Bruzual & S. Charlot ed., *IAU Symposium Vol. 262 of IAU Symposium, Evolution of binary stars and its implications for evolutionary population synthesis*. pp 44–47
- Han Z., Podsiadlowski P., Eggleton P. P., 1995, *MNRAS*, 272, 800
- Han Z., Podsiadlowski P., Lynas-Gray A. E., 2007, *MNRAS*, 380, 1098
- Hjellming M. S., Webbink R. F., 1987, *ApJ*, 318, 794
- Hurley J. R., Tout C. A., Pols O. R., 2002, *MNRAS*, 329, 897
- Lançon A., Gallagher III J. S., Mouhcine M., Smith L. J., Ladjal D., de Grijs R., 2008, *A&A*, 486, 165
- Le Borgne D., Rocca-Volmerange B., Prugniel P., Lançon A., Fioc M., Soubiran C., 2004, *A&A*, 425, 881
- Lee H., Worthey G., Dotter A., 2009, *AJ*, 138, 1442
- Leitherer C., Schaerer D., Goldader J. D., González Delgado R. M., Robert C., Kune D. F., de Mello D. F., Devost D., Heckman T. M., 1999, *ApJS*, 123, 3
- Lejeune T., Cuisinier F., Buser R., 1997, *A&A*, 125, 229
- Lejeune T., Cuisinier F., Buser R., 1998, *A&A*, 130, 65
- Li Z., Han Z., 2007, *A&A*, 471, 795
- Li Z., Han Z., 2008a, *MNRAS*, 387, 105
- Li Z., Han Z., 2008b, *ApJ*, 685, 225
- Li Z., Han Z., 2009, *Research in Astronomy and Astrophysics*, 9, 191
- Li Z., Mao C., Li R., Li M., 2010, *Research in Astronomy and Astrophysics*, 10, 135
- Maraston C., 2005, *MNRAS*, 362, 799
- Mármol-Queraltó E., Cardiel N., Sánchez-Blázquez P., Trager S. C., Peletier R. F., Kuntschner H., Silva D. R., Cenarro A. J., Vazdekis A., Gorgas J., 2009, *ApJ*, 705L, 199
- Mazeh T., Goldberg D., Duquennoy A., Mayor M., 1992, *ApJ*, 401, 265
- Mollá M., García-Vargas M. L., Bressan A., 2009, *MNRAS*, 398, 451
- Robert C., Pellerin A., Aloisi A., Leitherer C., Hoopes C., Heckman T. M., 2003, *ApJS*, 144, 21
- Salpeter E. E., 1955, *ApJ*, 121, 161
- Schulz J., Fritze-v. Alvensleben U., Möller C. S., Fricke K. J., 2002, *A&A*, 392, 1
- Thomas D., Maraston C., Bender R., Mendes de Oliveira C., 2005, *ApJ*, 621, 673
- Tout C. A., Aarseth S. J., Pols O. R., Eggleton P. P., 1997, *MNRAS*, 291, 732
- Van Bever J., Belkus H., Vanbeveren D., Van Rensbergen W., 1999, *NewA*, 4, 173
- Van Bever J., Vanbeveren D., 2000, *A&A*, 361, 1191
- Van Bever J., Vanbeveren D., 2003, *A&A*, 400, 63
- Vazdekis A., 1999, *ApJ*, 513, 224
- Vázquez G. A., Leitherer C., Schaerer D., Meynet G., Maeder A., 2007, *ApJ*, 663, 995
- Westera P., Lejeune T., Buser R., Cuisinier F., Bruzual G., 2002, *A&A*, 381, 524
- Yi S., Lee Y., Woo J., Park J., Demarque P., Oemler Jr. A., 1999, *ApJ*, 513, 128
- Yi S. K., Yoon S., Kaviraj S., et al. 2005, *ApJ*, 619, L111
- Zhang F., Han Z., Li L., Shan H., Zhang Y., 2010, *MNRAS*, 408, 1283